



## **Small, low-cost, and easy-to-use dip coating machine design and construction and analyse the performance of Green leaf extraction with TiO<sub>2</sub>**

**Revathi N<sup>a</sup>, Ali Fatima A<sup>b\*</sup>, Nagamani Prabu A<sup>c\*</sup>**

<sup>ab</sup> PG and Research Department of Physics, Government Arts College, Udumalpet, Affiliated Bharathiar, university Tamilnadu, 642126, India

<sup>c</sup>Center for Energy and Nano Research, Department of Physics, Karpagam Academy of Higher Education, Coimbatore, Tamilnadu, 641021 India

Corresponding Authors Email: [alif41070@gmail.com](mailto:alif41070@gmail.com), [prabhu.spectra@gmail.com](mailto:prabhu.spectra@gmail.com)

### **Abstract**

Dip coaters are a type of compact coating equipment that allows for the application of coatings that are uniform and consistent to a variety of substrates. This article explains a less expensive design for a dip coater that has requirements that are comparable to those of other dip coaters. The machine is made up of a DC 12V Motor, LED display with hall sensor, and a housing that is assembled out of wood and acrylic to prevent dust from settling on the substrate. Mechanical structure and electrical drive, which makes it simple to implement any necessary adjustments. Because of its compact design, the dip coater is ideally suited for use in laboratories. The vast majority of the components can be used in their purchased state without requiring any adjustments, which makes constructing and replacements simple tasks, along with this performance analysed through neem leaf extraction with Tio<sub>2</sub> Coated through proposed Dip coating Unit

**Keywords:** Dip coater, Mechanical Gear, Controller, wood casing, acrylic casing

### **Introduction**

Arash Abedijaberi et al. (2011) computationally study how viscoelasticity affects dip coating flow interfacial dynamics. The interfacial dynamics of air displacing a viscoelastic fluid

under gravity—dip coating flows—are examined. Computations use a stabilised finite element method and pseudo-solid domain mapping. FENE-CR models the fluid.

Abdelkader Filali et al. (2013) simulated dip coating Newtonian and Bingham fluids numerically. For Newtonian and Bingham fluids, the dip-coating process is simulated numerically to locate the free surface under different conditions. The simulations mainly evaluate the Finite-Volume Method (FVM) combined with the Volume-Of-Fluid (VOF) technique embedded in the commercial code (Fluent), but some results are also obtained with the Finite-Element Method (FEM) using another commercial code (Polyflow). Numerical results were validated against Newtonian limit experimental data. Coating fluid properties and surface withdrawal speed for Newtonian fluids and yield stress for Bingham fluids are considered.

David Loza et al. (2014) built a dip and spin coating device using cheap mechanical parts and open software. The spin coater's speed range is 500 to 10,000 rpm, and the dip coater's is 0.6 cm/h to 30 cm/min. These instruments outperform commercial models.

Martha A. Herrera et al. (2016) used spin- and dip-coating to create an environmentally friendly gas barrier on porous materials: nano cellulose coatings. Microscopy showed that spin-coating was suitable for smaller pore substrates and dip-coating for larger ones. Spin-coated layers were hundreds of nanometers thick, while dip-coated ones were micrometres. Coating thickness and roughness increased contact angle. NC coating had low oxygen permeability (between 0.12 and 24 mL/μm/(m<sup>2</sup> x 24 h x kPa)) at 23% RH, but at 50% RH it was too high to measure, except for the dip-coated sample with 23 μm thickness.

Karthika Muthukrishnan et al. (2016) studied sol–gel dip coated ZnO thin film acetone sensing. Zinc nitrate hexahydrate (Zn (NO<sub>3</sub>)<sub>2</sub> · 6H<sub>2</sub>O) and Na-CMC were used to synthesise dip coating sol. X-ray diffraction measured thin film crystallinity and crystallite size (XRD).

FESEM examined morphology (FESEM). Exposing the film to various acetone concentrations at room temperature using chemiresistive method studied gas sensing characteristics.

Jesswein et al. (2017) continuously dipped PVDF hollow fibre membranes in PVA for humidification. They Composite hollow fibre membranes for gas-to-gas humidification were tested for polymer electrolyte fuel cell external humidifiers (PEMFC). Thus, porous poly(vinylidene fluoride) (PVDF) hollow fibres were wet spun, coated with thin layers of polyvinyl alcohols (PVA) via continuous dip coating, and cross-linked by glutaraldehyde.

MiaoWang et al. (2017) structurally functionalized industrial softwood kraft lignin for simple dip-coating of urea as highly efficient nitrogen fertiliser. Dip-coating polylactic acid (PLA) with industrial softwood kraft lignin produced urea coating. Repeating the coating process increased coat thickness to 81% of the urea core.

Michinari Kohri et al. (2017) dip-coated biomimetic melanin-like particles with polydopamine shell layers to create bright structural colour films independent of background. We examined dip-coating parameters that affect structural coloration. The films had bright and angle-dependent structural colours regardless of background colour, black or white. These findings inform dye-free ink technology development.

Lilian Sarango et al. (2018) controlled MOF deposition by dip-coating in thin film Nano composite membranes for organic solvent nanofiltration. Dip-coating on polyimide P84® asymmetric supports deposited  $70 \pm 10$  nm and  $240 \pm 40$  nm ZIF-8 and ZIF-67 particles. This produces a MOF monolayer on the polyimide support during polyamide interfacial polymerization under ideal conditions. This simple method yields good OSN results: 90% dye rejection and  $8.7 \text{ L m}^{-2} \text{ h}^{-1} \text{ bar}^{-1}$  methanol permeance.

Dip coating aligned Ag nanowires on glass sheet by jinyang Feng et al. (2018). Dip-coating a Polyvinylpyrrolidone/ethanol solution on glass produced a thin film with highly-

oriented Ag nanowires. PVP concentration and pulling speed during dip-coating determine Ag nanowire alignment. The 1400–1900 nm wavelength range exhibits optical polarisation.

In the present, people have tried to make a small dip coating that doesn't need a lot of complicated code or algorithms. Coating is a by-product of thin-film technology. Commercially available dip coating costs are not affordable to users. In this consideration, we proposed a mechanical and electrical drive-based construction and design. This prototype was designed with locally available materials. And analysed its performance and through neem extracted dye with titanium oxide

### **Design construction and working of Compact dip coating unit**

Materials: Mechanical structure of dip coating unit consist of as followings

- |                                    |                          |                   |                                      |
|------------------------------------|--------------------------|-------------------|--------------------------------------|
| 1. 12 dc motor                     | 2. Helical rod with nut  | 3. Supporting rod | 4. Limit switch                      |
| 5. Limit switch                    | 6. Substrate holding rod | 7. Power switch   | 8. Digital display with Rpm Detector |
| 9. Helical rod holder with bearing | 10. Speed controller     |                   |                                      |

The dip coating unit is made up of two major components: a mechanical structure and an electrical drive. The mechanical structure is made of a linear actuator, which is a long screw with the right nut on the end. Mechanical structure of the proposed model is depicted in figure 1. The long screw axis has been connected to the 12 VDC motor. The regulator controls the motor's torque, and limit switching controls whether the motor turns clockwise or counter clockwise. How far apart the two limit switches are depends on how long you want the substrate to be coated. Limit switch action desired the action of up-and-down motion through electrical drive. Electrical drive schematic diagram has been depicted in figure 2.

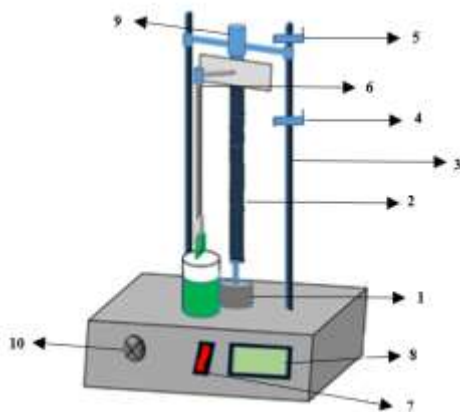


Figure 1. Schematic diagram of dip coating mechanical Structure

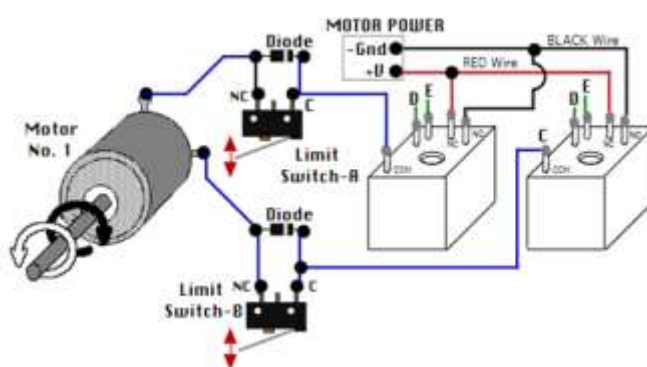


Figure 2. Schematic diagram of dip coating electrical drive

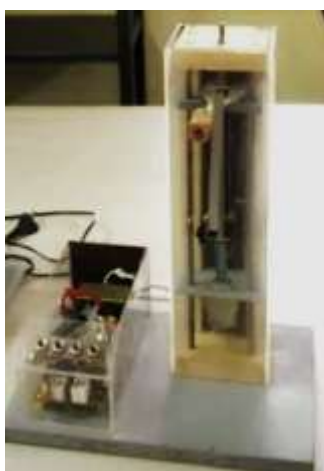


Figure 3. Photograph of proposed design of Dip coating unit

### **Preparation of substrate**

The chopped Neem leaves weighing 20 g were put in a 250 mL Erlenmeyer flask after being washed in distilled water. After boiling for five minutes, 100 millilitres of sterile, double-distilled water were added. Whatman Using No. 1 filter paper with a 25 m pore size, the leaf extract was purified and stored at 4 oC. To create titanium nanoparticles, 90 millilitres of 5 mM aqueous TiO<sub>2</sub> were combined with 10 millilitres of neem leaf broth. The following investigation is discussed. Titanium nanoparticles were refined by repeatedly centrifuging at 10,000 rpm for 10 minutes in double-distilled water and re-dispersion in deionized water. The resulting solution was coated on substrate through a proposed dip coating unit with 20 dips.

### **FTIR Spectroscopy**

FTIR spectroscopy identified chemicals that create and stabilise titanium nanoparticles. Fig. 4 exhibits FTIR spectra of Neem leaf extract and produced titanium nanoparticles. The FTIR spectra of neem leaf broth showed peaks at 3400.31, 2073.56, 1637.73, and 657.92 cm<sup>-1</sup>. Alcohols and phenolics stretch O–H at 3400.31. C=C vibrations are absorbed at 2073.56. The band at 657.92 is C–H bending, and the peak at 1637.73 is C=O stretching of amide I or C=C groups of aromatic rings. Terpenoids, flavonoids, and proteins in Neem leaf extracts were thought to produce and stabilise titanium nanoparticles. Prathna and Shankar<sup>13</sup> and <sup>14</sup> reported similar results.

Biosynthesized titanium nanoparticles had FTIR peaks at 3421.63, 1640.53, 1083.76, and 775.38 cm<sup>-1</sup>. The 3421.63 peak represents the O-H stretching of alcohols and phenolic compounds, whereas the 1637.73 peak represents the C=O stretching of amide I or aromatic rings. 1083.76 nm absorbs carboxylic acid and alcohol C-O vibrations. Yilmaz et al.<sup>16</sup> found the same. Titanium nanoparticles' 775 peak is connected with Ti-O-Ti stretching vibration. .

O-H stretching and the C=C group characterise Neem leaf extract terpenoid chemicals. Tripathy et al.<sup>18</sup> found that terpenoid compounds caused O-H stretching, C=C group in an aqueous extract of *Azadirachta indica* (Neem) leaves.

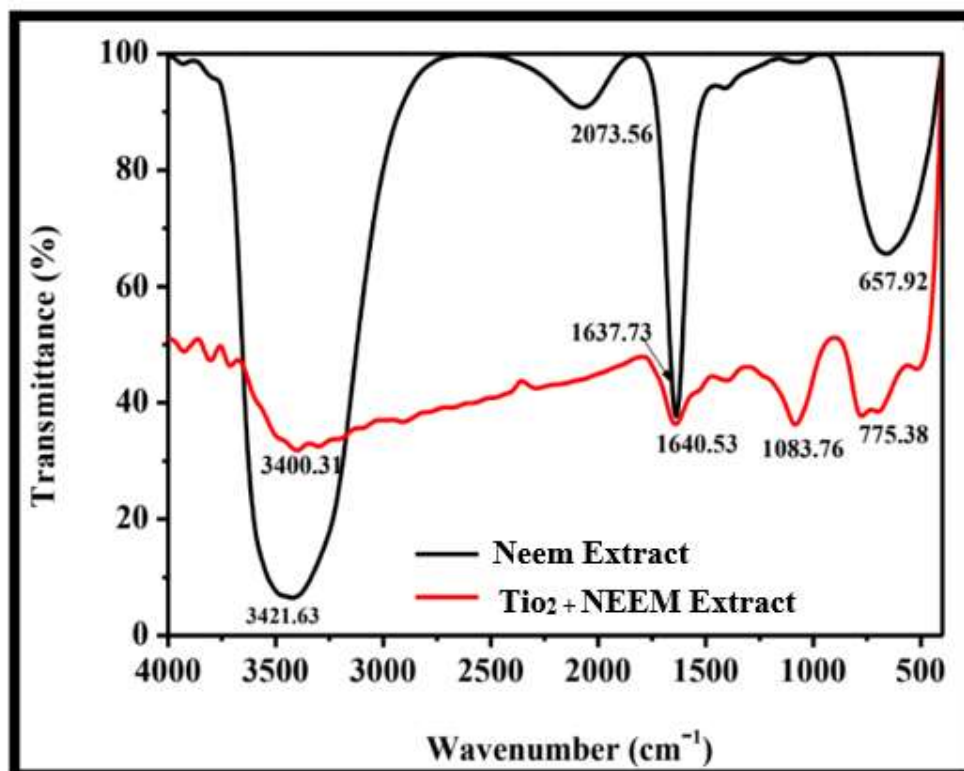


Figure 4. FTIR Spectra of Neem Leaf extract and TiO<sub>2</sub> with Neem Leaf Extract

#### FESEM and EDX analysis of titanium nanoparticles

FESEM showed that biosynthesized titanium nanoparticles were spherical and 25–87 nm in size (Fig. 5). EDS (Fig. 6) showed prominent titanium (Ti) peaks at 4.4 to 5 keV, silica (Si) at 1.8 keV, oxygen (O) at 0.6 keV, and carbon (C) at 0.2 keV. Film preparation or EDS detector glass substrate caused the Si peak. Titanium nanoparticles' C peak showed biomolecules.

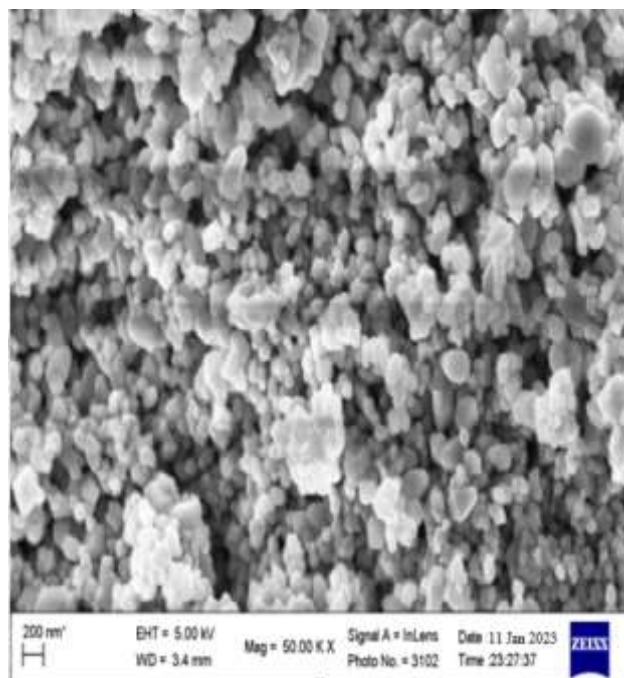


Figure 5. SEM image of titanium nanoparticles,

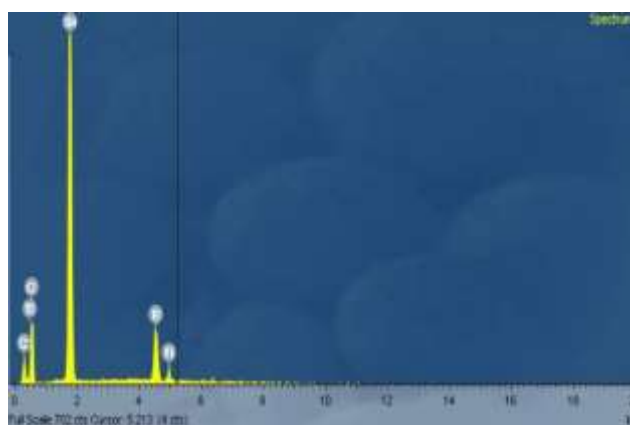


Figure 6. EDAX spectrum of titanium nanoparticles

### **Hazard Free**

No risk of electrical shock exists due to the low voltage (12 V, 0.5 A) used in the dip-circuits. Coater's Still, all cables and electrical components have been isolated with electrical tape for further safety. The pinewood frame and other parts of the apparatus are flammable and must be treated with care and stored in a fireproof location. The dip-coater needs a flat, level



surface to sit on. We advise securing the beaker with the precursor solution to the apparatus so that no spills occur. At the end of the day, it's best to handle it while outfitted in safety gear.

## **Conclusion**

The production of a dip coating apparatus on a low budget was a success. Dip coating equipment is capable of working with both glass and silicon substrates. Because the equipment has an electrical drive, producing thin films requires significantly less effort. The use of low-cost components allows for the creation of a product that is both lightweight and convenient. It is clear that wood was utilized in the building, indicating that the object is strong and well-made. Fully designed and built like an automatic machine, it prepared the solution and evenly coated the glass substrate.

## **Reference**

1. Arash Abedijaberi, Gandharv Bhatara, Eric S. G. Shaqfeh, Bamin Khomami. A computational study of the influence of viscoelasticity on the interfacial dynamics of dip coating flow, July 2011, Journal of Non-Newtonian Fluid Mechanics 166(12-13):614-627: 10.1016/j.jnnfm.2011.03.002
2. Abdelkader Filali, Lyes Khezzar, Evan Mitsoulis, Some experiences with the numerical simulation of Newtonian and Bingham fluids in dip coating, April 2013, Computers & Fluids 82:110-121: 10.1016/j.compfluid.2013.04.024.
3. David Loza, Victor Hugo Guerrero, Reza Dabirian, Construction of low cost spin and dip coaters for thin film deposition using open source technology, December 2014, License, CC BY-ND 4.0.
4. Martha A. Herrera, Juho Sirviö, Aji P Mathew, Kristiina Oksman, Environmental friendly and sustainable gas barrier on porous materials: Nanocellulose coatings prepared using spin- and dip-coating, December 2015, Materials and Design 93.10.1016/j.matdes.2015.12.127
5. Karthika Muthukrishnan, Manoj Vanaraja, Shanmugam Boomadevi, Rakesh Kumar Karn, Vijay Singh, Pramod K. Singh, Krishnamoorthy Pandiyan, Studies on acetone sensing characteristics of ZnO thin film prepared by sol-gel dip coating. <https://www.inфона.pl/resource/bwmetal.element.elsevier-c1a4a8d3-92af-387d-88f1-639a0e74de37/tab/contributors>.
6. Jesswein, T. Hirth, Thomas Schiestel Continuous dip coating of PVDF hollow fiber membranes with PVA for humidification, July 2017, Journal of Membrane Science 541. 10.1016/j.memsci.2017.07.010.
7. Michinari Kohri, Shigeaki Yamazaki, Ayaka Kawamura, Tatsuo Taniguchi Bright structural color films independent of background prepared by the dip-coating of biomimetic melanin-like particles having polydopamine shell layers. March 2017. Colloids and Surfaces A Physicochemical and Engineering Aspects 532. 10.1016/j.colsurfa.2017.03.035.
8. Lilian Sarango, Lorena Paseta, Marta Navarro, Beatriz Zornoza, Joaquín Coronas, Controlled deposition of MOFs by dip-coating in thin film nano composite membranes for organic solvent nano filtration. Journal of Industrial and Engineering Chemistry. Volume 59, 25 March 2018, Pages 8-16. 10.1016/j.jiec.2017.09.053.
9. Jinyang Feng, Huida Xia, Fangfang You, Haibo Mao, Xiao Ma, Haizheng Tao, Xiujuan Zhao, Moo-Chin Wang. Alignment of Ag nanowires on glass sheet by dip-coating technique. Journal of Alloys and Compounds, Volume 735, 25 February 2018, Pages 607-612. 10.1016/j.jallcom.2017.09.154..